NASA TECHNICAL MEMORANDUM

NASA TM X-3074

NASA TM X-3074

FLYOVER NOISE CHARACTERISTICS OF A TILT-WING V/STOL AIRCRAFT (XC-142A)

by Robert J. Pegg, Herbert R. Henderson, and David A. Hilton

Langley Research Center
Hampton, Va. 23665

NATIONAL AERONAUTICS AND SPACE ADMINISTRATION • WASHINGTON, D. C. • AUGUST 1974

1. Report No. NASA TM X-3074	2. Government Accession No.	3. Recipient's Catalog No.
4. Title and Subtitle FLYOVER NOISE CHARACTERISTICS OF A TILT-WING V/STOL AIRCRAFT (XC-142A)		5. Report Date August 1974 6. Performing Organization Code
7. Author(s) Robert J Pegg, Herbert R. Henderson, and David A Hilton		8. Performing Organization Report No. L-9037
9. Performing Organization Name and Address NASA Langley Research Center Hampton, Va 23665		10. Work Unit No. 501-24-12-02 11. Contract or Grant No.
12. Sponsoring Agency Name and Address National Aeronautics and Space Administration Washington, D.C 20546		13. Type of Report and Period Covered Technical Memorandum 14. Sponsoring Agency Code
15. Supplementary Notes		

16. Abstract

A field noise measurement investigation was conducted during the flight testing of an XC-142A tilt-wing V/STOL aircraft to define its external noise characteristics Measured time histories of overall sound pressure level show that noise levels are higher at lower airspeeds and decrease with increased speed up to approximately 160 knots The primary noise sources were the four high-speed, main propellers Flyover-noise time histories calculated by existing techniques for propeller noise prediction are in reasonable agreement with the experimental data

17. Key Words (Suggested by Author(s)) Aircraft Noise Propellers		18. Distribution Statement Unclassified – Unlimited STAR Category 02	
19. Security Classif. (of this report) Unclassified	20. Security Classif. (of this page) Unclassified	21. No. of Pages 24	22. Price* $3.00

*For sale by the National Technical Information Service, Springfield, Virginia 22151

FLYOVER NOISE CHARACTERISTICS OF A TILT-WING V/STOL AIRCRAFT (XC-142A)

By Robert J. Pegg, Herbert R. Henderson,
and David A. Hilton
Langley Research Center

SUMMARY

A field noise measurement investigation was conducted during the flight testing of a large V/STOL, tilt-wing aircraft to define its external noise characteristics. Measured time histories of overall sound pressure level show that noise levels are higher at lower airspeeds and decrease as the speed is increased up to approximately 160 knots. The primary noise sources were the four high-speed, main propellers. Flyover-noise time histories calculated by means of existing techniques for propeller noise prediction are in reasonable agreement with the experimental data. There appears to be an increasing discrepancy between the measured and calculated noise with increasing thrust-axis angle; this is believed to be due to unsteady blade loading associated with the high angles of attack at which the propellers operate.

INTRODUCTION

Several design approaches to obtaining V/STOL operating characteristics for commercial aircraft have been proposed. One such approach is the propeller-driven, tilt-wing vehicle typified by the XC-142A aircraft. Among the questions associated with the operation of such a vehicle are its noise characteristics in the terminal area environment. Propeller orientation and operating conditions vary as a function of airspeed; hence, the far-field noise pattern can be expected to vary considerably with time and aircraft position relative to the observer.

Predictions of noise produced by propeller-driven, tilt-wing V/STOL aircraft are complicated by the wide angle-of-attack operating range of the propellers, which are the predominant noise source. The mechanisms that influence propeller-noise radiation patterns have been advanced in reference 1, which extends Gutin's steady-loading concept for static conditions to an axially moving propeller. In addition, existing rotor and propeller theory (ref. 2) has shown the importance of higher harmonic air loads on the radiated noise. However, few data on very high-frequency loading exist for propellers at high angles of attack. The wind-tunnel data of reference 3 for tilt-rotor aircraft would provide an initial starting point from which theoretical noise calculations could be made. The conventional empirical methods (ref. 4) for predicting propeller noise, however, do not include the effects of high-frequency fluctuating blade loads.

Because of the concern for noise impact of V/STOL aircraft and the lack of adequate prediction methods, a noise measurement program was undertaken on an XC-142A tilt-wing aircraft to determine its noise characteristics in forward flight. The far-field noise properties of the aircraft while hovering had been previously reported in reference 5. Also, the noise characteristics of a single propeller of the type used on the aircraft, as measured statically, are described in reference 6. The acoustic measurements herein were taken from a five-microphone array located along the flight path, approximately 90 m below the aircraft. The results are compared with values of flyover noise predicted by the theory of reference 4, which is representative of the state of the art for propeller-driven aircraft.

NOMENCLATURE

B	number of blades
dBA	A-weighted sound pressure level, dB (re: 20 $\mu N/m^2$)
EPNL	effective perceived noise level
PNL	perceived noise level
m	order of harmonic
max.	maximum
MR	main propeller
OASPL	overall sound pressure level
TR	tail propeller

TEST AIRCRAFT AND PROCEDURES

Test Aircraft

The test aircraft was a combination tilt-wing, deflected-slipstream V/STOL vehicle with a gross weight of about 17 250 kg. Power was supplied by four T64 turboshaft engines with a combined output of about 9.20 MW. The engines, linked by cross-shafting, were located in wing-mounted nacelles and drove four 4.77-m-diameter propellers and a three-bladed tail propeller. The function of the tail propeller was to provide longitudinal control in hover. The wing was equipped with leading-edge slats, located behind the upgoing side of the propellers, and full-span, double-slotted flaps located on the trailing edge. The main and tail propellers were geared together. In normal operation the tail propeller was disengaged and stopped at an airspeed between 100 and 120 knots. Some of the principal physical characteristics of the test aircraft are given in table I. A photograph of the test aircraft in the hover flight mode is presented in figure 1, and a three-view drawing is shown in figure 2. For the particular aircraft used in this investigation, figure 3 shows the variation of wing incidence angle (inclination angle of propeller thrust axis) and power loading with airspeed. Further information on the configuration and operational characteristics of this vehicle may be found in references 5, 7, and 8.

Test Conditions

The test area was located in a region where the surface condition is flat with a cut-grass ground cover. Five microphones in a cross array, shown in figure 4, were used to obtain the noise measurements. All flyover noise measurements were made with the aircraft flying a heading which took it directly over microphones 1, 3, and 5. During the noise-data recording periods the surface wind velocity was 10 knots or less, as recommended in reference 9. Altitude and airspeed were recorded from the cockpit instrumentation. Table II lists the various flight conditions and pertinent aircraft operating parameters, such as propeller speed and wing angle. The weight of the test aircraft varied from 16 900 kg at the start of the mission to approximately 15 350 kg at the end of the tests.

Noise-Measurement Equipment

A schematic diagram of the data acquisition system is shown in figure 5. The microphones are commercially available, piezoelectric ceramic type with a frequency range of 20 to 12 000 Hz. The microphones were mounted 1.5 m above the ground with their axis oriented in such a manner as to afford approximate grazing incidence at all times. The signal outputs from all microphone systems were recorded on multichannel, frequency-modulated magnetic tape recorders at 76.2 cm/sec and a center frequency of 54 kHz. The frequency response of the complete recording system was flat, to within ±3 dB, from 20 to 12 000 Hz.

The entire sound-measurement system was calibrated in the field prior to and after completion of the flights by means of a sound-level calibrator employing a 1000-Hz sine wave signal and a sound pressure level of 114 dB. Real-time synchronization between all microphone positions was achieved by recording standard IRIG-B time code format on one channel of the magnetic tape.

RESULTS AND DISCUSSION

The estimated airplane operating conditions, based on cockpit instruments, are presented for each run of the investigation in table II. The maximum overall sound pressure levels and 1/3-octave-band levels for the indicated flight conditions are given for each microphone position and each run in table III. The noise data in dBA, PNL, and EPNL are also given for each run in this table. The measured noise data presented in this table have not been normalized to a given distance nor to reference atmospheric conditions. The results discussed in the following sections are presented in the form of flyover-noise time histories, 1/3-octave-band spectra, narrow-band spectra, and overall sound pressure levels.

The ambient noise spectrum in the test area is given in figure 6. Most of the noise energy is contained in the bands centered at 63 Hz, where the level was approximately 64 dB. These ambient noise levels are considerably lower than the aircraft noise levels encountered during the test program.

Flight-Test Results

Narrow-band frequency analyses (4 Hz bandwidth) were made from data taken while the aircraft moved at an airspeed of approximately 10 knots and an altitude of approximately 79 m (run 8). Shown in figure 7 are the narrow-band spectra for positions underneath, as well as forward and aft of, the aircraft; some of the noise peaks due to the main propeller and tail propeller are identified as aids in the interpretation. The principal noise components for this particular aircraft were found to be at frequencies below 1000 Hz and are identified with the main propellers. A secondary source of noise is the pitch-control tail propeller. Other noise sources such as the engine compressor, exhaust, and gearing were not apparent in the data. From this figure, a significant change in the harmonic content of the main-propeller noise with position is observed; that is, the main-propeller tones have a lower amplitude aft of the aircraft.

The effects of forward speed and propeller thrust-axis angle are shown in figure 8. These time-history plots show the overall sound pressure levels during flyovers at various airspeeds and an altitude corrected to 91 m. The data as shown were measured at microphone 1 and are alined so that the maximum noise occurs at zero time. Sound pressure levels are seen to increase as the aircraft approaches, reach a maximum as the aircraft passes overhead, and decrease rapidly as the aircraft passes beyond the measuring position. Three airspeeds are shown in this figure; the slower airspeeds represent higher propeller thrust-axis angles and thus a more asymmetric propeller inflow. Also, the slower airspeeds produce higher maximum overall sound pressure levels and higher overall sound pressure levels during approach. As would be expected, the directional noise characteristics of the propellers in high-speed flight resemble those of conventional airplanes; in low-speed flight, those of a helicopter.

The spectral contents of the noise data shown in figure 8 are presented in figure 9 for three airspeeds and three time periods: 10 sec before overhead, overhead, and 5 sec after overhead. From figure 9(a) it can be seen that the higher airspeeds (and the lower thrust-axis inclination angles) have the lowest noise levels above 200 Hz. At frequencies below 200 Hz, the sound pressure levels are relatively insensitive to airspeed. These results are not as clearly defined in figures 9(b) and 9(c), but the same trend exists. It is significant to note that for a given time, considerable difference in aircraft distance from these microphones exists. This implies different noise radiation patterns for the various airspeeds.

Figure 10 presents the maximum overall sound pressure levels for the test aircraft during flyovers at different airspeeds and an altitude corrected to 91 m. The figure shows a gradual dropoff of maximum sound pressure level with airspeed, approximately 1 dB for every 10 knots of forward speed. This reduction is accounted for by the fact that as airspeed increases, propeller thrust angle decreases, power decreases, and propeller rotational speed varies slightly.

Comparison of Measured and Predicted Results

The empirical technique for propeller noise prediction outlined in reference 4, which is based on experimental data from numerous conventional propeller systems, was used to calculate far-field noise values, which are compared with the time histories from figure 8. These comparisons are shown in figures 11(a) and (b), where it is observed that (a) the shapes of the measured and calculated time histories are similar, which implies that the noise directivity patterns for propellers operating with conventional inflow conditions approximate those for propellers operating at high angles of attack, and (b) the absolute values of the computed noise-level time histories are approximately the same as the measured values for the high-speed case (axial inflow) and are approximately 8 to 10 dB less than the measured data for the low-speed case. This discrepancy in sound pressure level may be due to the higher disk loading and unsteady inflow at the higher tip Mach numbers. Other sources of unsteady blade loading contributing to the high noise levels are the high angles of attack and the overlapped condition at which the propellers were operating.

CONCLUDING REMARKS

A field noise measurement program was conducted on an XC-142A tilt-wing V/STOL aircraft. The purpose of this study was to document and perform a limited analysis on the noise characteristics of the test aircraft during flyover operations at incremental airspeeds between 10 knots and 160 knots.

An analysis of the measured results shows that the high-speed main propellers are the predominate noise source from this aircraft. A secondary noise source was identified as the pitch-control tail propeller. The aircraft at the slower airspeeds (higher thrust-axis inclination angle) produces the highest overall noise levels and higher sound pressure levels during the approach phase of the flyover operation. In all cases, the noise dropped off rapidly after the aircraft passed overhead. Flyover-noise time histories predicted with an existing empirical method were in good agreement with the experimental data. However, at low airspeeds the measured and calculated overall sound pressure levels show some difference, which is believed to be due to unsteady blade loading primarily associated with the high angles of attack at which the propellers operate. Maximum overall noise levels decrease with airspeed at approximately 1 dB per 10 knots because of reduced power required, lower propeller rotational speeds, and a more axially symmetric inflow.

Langley Research Center,
National Aeronautics and Space Administration,
Hampton, Va., June 7, 1974

REFERENCES

1. Garrick, I. E.; and Watkins, Charles E.: A Theoretical Study of the Effects of Forward Speed on the Free-Space Sound-Pressure Field Around Propellers. NACA Rep. 1198, 1954. (Supersedes NACA TN 3018.)
2. Lowson, M. V.; and Ollerhead, J. B.: A Theoretical Study of Helicopter Rotor Noise. J. Sound & Vib., vol. 9, no. 2, Mar. 1969, pp. 197-222.
3. Schmitz, F. H.; Stepniewski, W. Z.; Gibs, J.; and Hinterkeuser, E.: A Comparison of Optimal and Noise-Abatement Trajectories of a Tilt-Rotor Aircraft. NASA CR-2034, 1972.
4. Munch, Charles L.: Prediction of V/STOL Noise for Application to Community Noise Exposure. Rep. No. DOT-TSC-OST-73-19, U.S. Dep. Transportation, May 1973.
5. Hancock, R. N.: External Noise and Downwash Measurements on the Vought XC-142A. Proceedings of the Joint Symposium on Environmental Effects on VTOL Designs, Amer. Helicopter Soc., Inc., 1970.
6. Metzger, Frederick B.: A Study of Propeller Noise Research. Aerodynamic Noise, Univ. of Toronto Press, c.1969, pp. 371-386.
7. Kelley, Henry L.; and Champine, Robert A.: Flight Investigation of a Tilt-Wing VTOL Aircraft in the Terminal Area Under Simulated Instrument Conditions. AIAA Paper No. 71-7, Jan. 1971.
8. Ransome, Robin K.; and Jones, Gay E.: XC-142A V/STOL Transport Tri-Service Limited Category 1 Evaluation. FTC-TR-65-27, U.S. Air Force, Jan. 1966. (Available from DDC as AD 477 084.)
9. Anon.: Measurements of Aircraft Exterior Noise in the Field. ARP 796, Soc. Automot. Eng., Inc., June 15, 1965.

TABLE I.- AIRCRAFT DIMENSIONS AND CHARACTERISTICS

General:	
Wing span, m	20.57
Length, m	17.68
Normal gross weight, kg	17 250
Power (four T64 turboshaft engines), kW	2300
Wing area, m^2	49.6
Aspect ratio	8.53
Propellers:	
Main:	
Diameter, m	4.76
Design rotational speed, rpm	1232
Design tip speed, m/sec	307
Activity factor	91
Disk area (each), m^2	17.8
Number of blades	4
Tail:	
Diameter, m	2.44
Design rotational speed, rpm	2400
Design tip speed, m/sec	307
Activity factor	150
Disk area, m^2	4.69
Number of blades	3

TABLE II.- SUMMARY OF OPERATING CONDITIONS

[All runs made in trim, unaccelerated, level flight]

Run	Altitude, m	Wing angle, deg	Flap deflection, deg	Main propeller speed, % design rpm	Airspeed, knots	Power, MW	Estimated gross weight, kg	Tail rotor
1	53	0	0	76	160	2.83	16 900	Off
2	98	0	20	88	140	3.28	16 800	Off
3	101	5	48	88	90	3.13	16 200	On
4	91	10	60	89	70	3.58	16 100	↓
5	90	20	60	89	45	3.88	16 000	↓
6	76	40	60	90	25	5.22	15 900	↓
7	85	60	35	89	20	5.97	15 700	↓
8	79	80	7	93	10	6.00	15 500	↓
9	---	10	60	93	70	3.65	15 400	↓
10	91	40	60	93	20	5.81	15 350	↓

TABLE III.- SUMMARY OF MAXIMUM NOISE DATA FOR XC-142A AIRCRAFT AS MEASURED ON-TRACK AND LATERALLY FOR VARIOUS FLIGHT CONDITIONS, ALTITUDES, AND FORWARD SPEEDS[1]

Run	Microphone	Sound pressure level, dBA	PNL, dB	EPNL, dB	Max. OASPL, dB	1/3-octave-band sound pressure level, dB, at center frequency of –																														
						10 Hz	12 Hz	16 Hz	20 Hz	25 Hz	32 Hz	40 Hz	50 Hz	63 Hz	80 Hz	100 Hz	125 Hz	160 Hz	200 Hz	250 Hz	320 Hz	400 Hz	500 Hz	630 Hz	800 Hz	1 kHz	1.25 kHz	1.6 kHz	2 kHz	2.5 kHz	3.2 kHz	4 kHz	5 kHz	6.3 kHz	8 kHz	10 kHz
1	1	92.3	110.66	103.65	105.0	62	68	73	71	77	77	76	86	86	84	92	91	79	88	88	85	88	87	83	81	80	73	79	72	71	75	69	67	69	71	77
1	2	85.0	103.86	98.65	98.1	64	70	69	64	75	71	76	95	87	77	89	86	88	77	79	77	81	81	77	73	71	72	67	70	69	65	63	64	63	64	64
1	3	92.3	111.14	103.91	105.4	64	62	72	61	73	74	83	85	89	83	99	93	86	90	93	88	87	82	81	76	74	78	77	72	72	69	67	66	68	74	77
1	4	86.8	104.40	99.52	98.3	64	70	73	68	73	68	81	95	89	78	88	85	88	82	87	78	84	80	79	78	72	75	69	70	67	67	66	66	65	67	66
1	5	87.0	102.67	96.03	97.3	50	50	56	56	55	69	57	67	88	72	84	93	87	89	79	89	81	73	77	73	72	71	69	68	66	66	65	64	64	69	66
2	1	101.6	116.83	110.30	108.8	61	62	62	72	70	67	76	73	74	99	97	84	92	99	92	95	99	97	96	91	84	79	77	79	76	75	71	69	68	72	70
2	2	98.9	114.89	106.87	108.1	61	59	59	71	67	68	71	69	82	90	83	91	92	98	94	83	90	90	88	82	83	81	78	76	74	73	72	69	68	76	69
2	3	102.3	115.87	109.23	108.4	60	61	66	72	71	72	77	66	83	96	83	93	97	97	99	95	97	98	95	90	85	80	81	81	77	76	72	71	69	75	73
2	4	98.9	113.56	106.71	106.8	59	60	63	76	68	70	76	68	80	90	87	91	98	92	93	95	96	92	91	83	81	80	77	76	73	73	70	72	71	74	71
2	5	98.8	114.64	109.09	107.0	59	60	67	72	68	66	75	71	73	98	95	84	91	97	90	91	98	94	90	88	81	76	76	76	77	73	71	69	68	74	73
3	1	102.4	111.50	112.91	110.7	61	62	62	73	64	74	74	67	76	97	83	94	98	96	94	92	91	93	95	92	86	80	77	77	75	74	72	70	67	73	69
3	2	100.3	114.63	110.01	108.0	60	61	61	70	64	77	68	69	89	91	89	91	99	99	93	95	96	92	95	90	85	82	77	77	77	76	75	73	72	74	69
3	3	100.4	114.62	111.13	109.0	62	62	61	74	67	74	74	66	80	97	86	97	94	97	94	97	94	93	88	86	90	81	77	77	71	70	72	69	67	73	70
3	4	97.6	112.52	108.70	106.7	59	61	64	76	66	76	74	69	93	91	89	94	98	99	98	92	97	92	83	82	83	80	75	75	75	77	74	71	71	75	72
3	5	101.3	116.01	111.79	110.6	61	59	62	72	67	78	73	69	74	97	81	94	98	98	93	93	99	93	92	91	83	84	77	75	73	71	71	69	66	72	70
4	1	102.6	117.07	113.56	110.5	61	62	65	75	68	75	77	68	76	99	95	98	96	96	94	97	97	90	94	93	87	82	81	79	78	76	73	69	67	72	69
4	2	101.6	117.16	112.03	110.2	59	60	62	70	64	74	72	71	99	95	90	98	98	92	99	97	96	96	96	94	90	87	85	81	80	79	76	74	72	74	70
4	3	103.8	116.84	112.77	110.7	61	61	63	76	66	78	70	66	76	97	98	90	98	98	96	94	97	97	95	93	93	89	81	81	76	73	70	70	69	73	70
4	4	101.9	116.12	111.01	109.6	59	62	61	71	69	76	69	69	82	98	84	94	94	98	96	97	92	96	93	93	90	83	80	78	76	76	74	74	72	73	72
4	5	103.0	117.27	114.17	110.7	61	62	63	75	69	68	77	68	77	98	95	98	96	97	95	98	97	94	96	95	92	86	81	80	78	74	71	68	78	73	69
5	1	111.4	126.31	122.33	117.1	61	64	76	86	74	73	77	73	99	95	91	98	97	97	96	94	95	92	93	91	98	97	94	94	92	93	91	84	87	84	81
5	2	107.3	121.24	118.41	113.5	60	64	70	80	71	72	74	75	89	90	90	98	99	92	96	97	94	92	99	98	96	93	94	91	92	87	81	84	78	78	72
5	3	108.6	123.10	120.56	115.0	63	66	80	85	73	78	81	74	90	96	99	93	99	95	99	92	97	92	91	99	98	95	95	95	92	88	82	79	75	78	78
5	4	106.9	120.76	118.86	113.9	61	62	77	94	75	73	83	73	96	95	96	98	99	92	93	99	96	93	98	97	94	94	91	89	84	82	80	78	83	78	77
5	5	109.5	123.81	120.88	115.6	62	65	73	87	75	71	73	69	80	99	98	90	99	93	91	94	95	94	90	99	90	95	96	94	91	88	84	85	77	76	73
6	1	114.9	128.75	127.45	121.4	65	67	75	86	78	78	80	82	96	97	99	96	92	90	91	94	96	92	97	95	93	92	90	95	94	96	88	85	83	93	83
6	2	117.8	125.67	124.50	117.8	65	72	75	83	77	75	74	74	74	84	83	93	94	99	92	93	96	99	99	96	96	93	91	88	85	84	81	80	79	80	76
6	3	114.5	127.95	127.28	120.6	67	68	75	86	76	74	82	74	79	96	88	93	97	96	92	91	92	98	90	94	92	90	90	96	87	86	83	82	74	81	78
6	4	113.1	127.68	125.84	120.6	71	73	72	83	79	75	76	74	99	99	94	94	95	90	96	92	91	93	92	92	98	99	91	92	87	84	83	78	74	78	76
6	5	109.6	123.33	122.33	117.2	65	66	64	70	65	67	73	76	94	91	87	88	92	99	91	99	93	94	91	98	96	97	93	83	82	79	78	77	73	78	76
7	1	114.9	128.81	129.41	120.5	68	72	74	76	77	76	82	74	91	97	97	94	92	92	93	99	93	91	96	92	92	91	90	99	94	95	93	86	81	83	83
7	2	109.4	124.98	125.95	118.4	65	65	65	70	65	76	79	74	87	94	85	94	97	91	90	98	93	94	92	90	96	94	89	86	83	82	79	78	77	79	75
7	3	114.6	127.91	128.09	119.3	67	67	73	84	71	73	79	72	98	95	95	96	94	91	92	93	96	91	97	94	93	93	99	91	97	94	92	89	85	85	84
7	4	107.5	122.27	124.78	114.9	67	69	72	80	73	72	78	74	92	99	93	99	95	96	98	98	92	91	99	90	97	95	92	86	85	84	81	80	78	80	79
7	5	113.6	127.67	128.29	119.4	68	68	70	77	70	76	82	75	94	99	98	98	92	94	91	91	96	90	94	93	92	91	96	97	95	95	86	82	80	82	81
8	1	114.2	127.36	123.74	120.1	70	69	68	76	73	79	82	75	89	98	97	95	96	98	96	93	96	99	98	92	90	92	97	93	91	90	85	84	83	82	84
8	2	109.6	125.66	124.78	116.1	77	75	69	79	73	75	78	73	79	96	84	95	99	90	91	92	92	97	96	92	93	94	92	90	94	94	84	83	83	84	82
8	3	115.9	130.39	130.05	121.8	70	71	71	82	77	79	82	74	86	98	96	95	91	99	99	93	97	91	99	97	94	91	90	90	92	90	88	84	79	86	82
8	4	99.3	117.67	118.75	112.1	79	83	91	97	94	98	90	91	91	91	96	98	99	92	99	92	93	89	89	87	86	84	80	78	75	74	75	73	72	72	77
9	1	109.6	123.33	117.69	115.6	61	64	68	76	69	77	76	67	80	92	96	91	96	96	91	90	93	93	94	98	97	95	92	92	89	90	89	80	78	78	76
9	2	107.9	122.55	116.37	114.2	61	62	60	68	67	80	74	68	77	97	82	96	90	97	98	98	95	97	91	99	96	95	93	90	91	91	88	85	84	82	73
9	3	108.0	122.46	116.27	115.0	60	61	62	78	68	76	76	71	77	90	91	99	99	98	91	94	93	90	91	97	96	92	89	86	84	83	87	83	74	76	75
9	4	109.3	124.41	116.40	115.5	60	59	62	76	66	79	74	68	83	94	92	96	98	98	92	97	94	95	91	91	97	96	94	91	90	85	80	85	77	86	84
9	5	108.5	123.55	117.03	115.2	61	62	64	77	66	83	77	71	76	90	93	90	99	98	91	92	95	99	90	98	99	94	87	89	86	82	87	77	72	75	74
10	1	112.8	126.54	126.91	117.8	69	70	72	83	70	76	77	72	88	95	98	92	90	99	94	95	90	96	93	91	90	90	97	98	96	93	85	83	81	80	81
10	2	112.7	127.20	125.75	119.0	66	68	68	76	74	77	77	73	89	98	89	91	92	93	94	90	93	94	91	91	90	98	99	94	95	87	90	79	79	82	83
10	3	113.5	127.09	126.05	117.9	64	67	68	77	71	77	78	71	87	94	93	98	95	96	94	95	90	93	99	92	91	91	90	97	95	86	84	83	80	85	89
10	4	112.5	127.50	126.52	119.0	69	69	71	80	76	81	80	71	80	93	83	91	94	91	98	94	97	90	91	93	99	96	92	88	92	86	84	79	77	76	75
10	5	109.5	122.38	122.05	114.6	66	64	64	73	67	68	73	70	68	86	80	91	90	97	96	93	96	94	93	90	90	99	91	86	83	82	81	78	74	76	75

[1]See table II for flight conditions.

L-68-10 461

Figure 1.- Test aircraft in hovering flight.

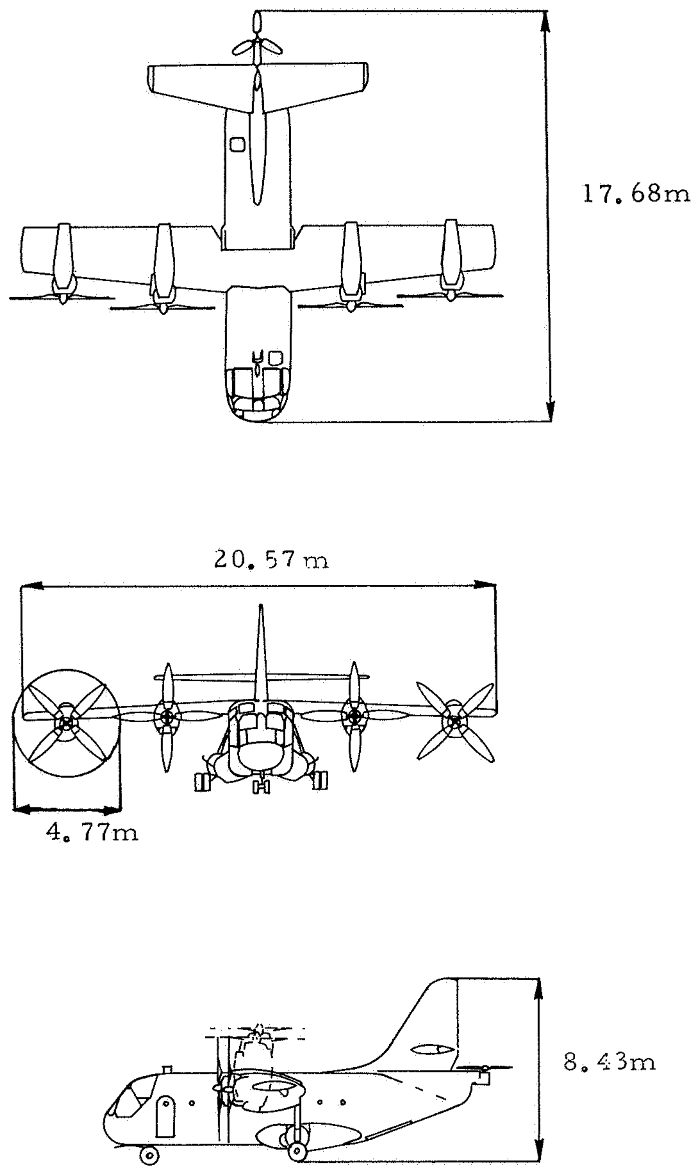

Figure 2.- Three-view drawing of test aircraft.

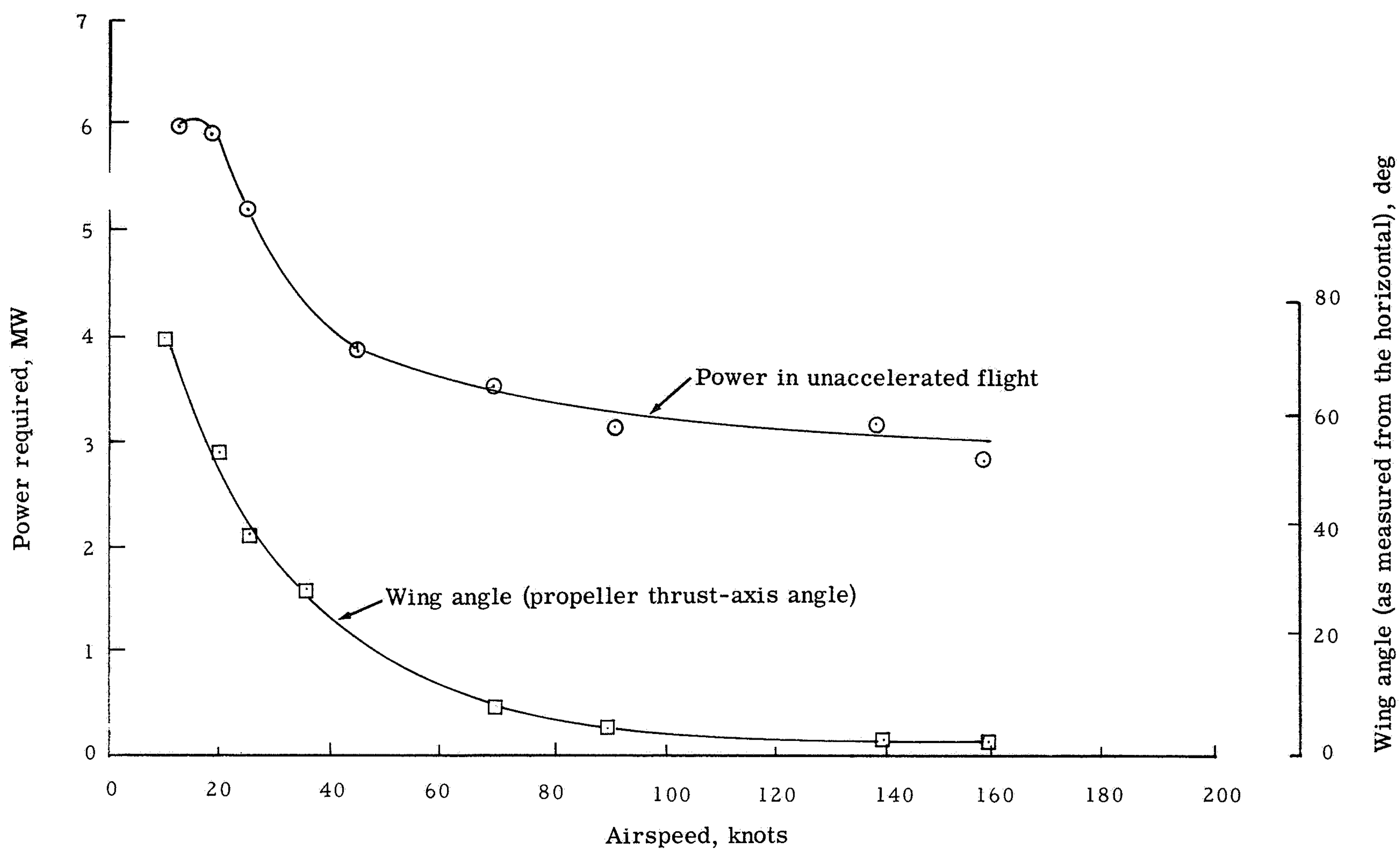

Figure 3.- Variation of power loading and wing angle with airspeed.

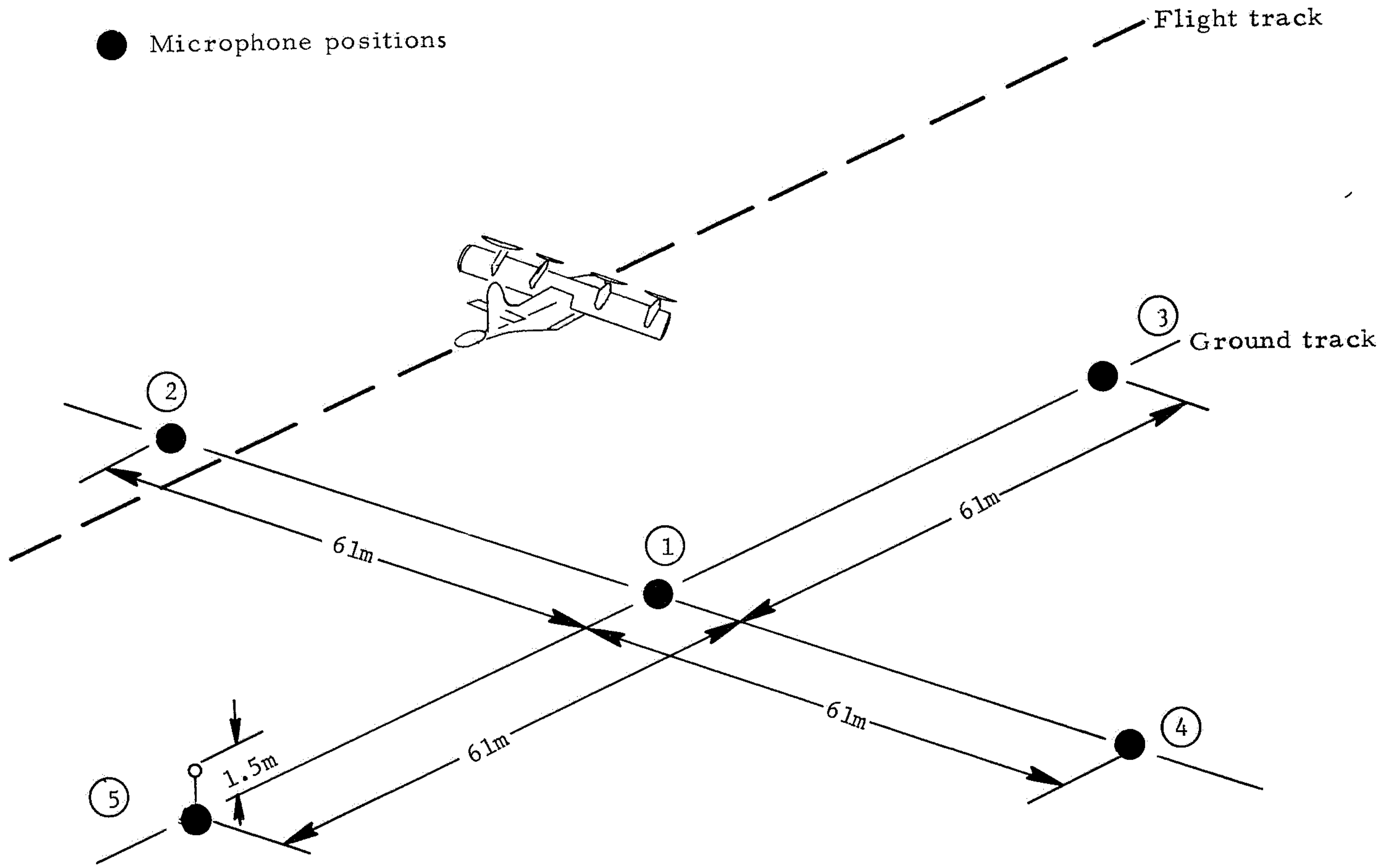

Figure 4.- Microphone layout for ground noise measurements.

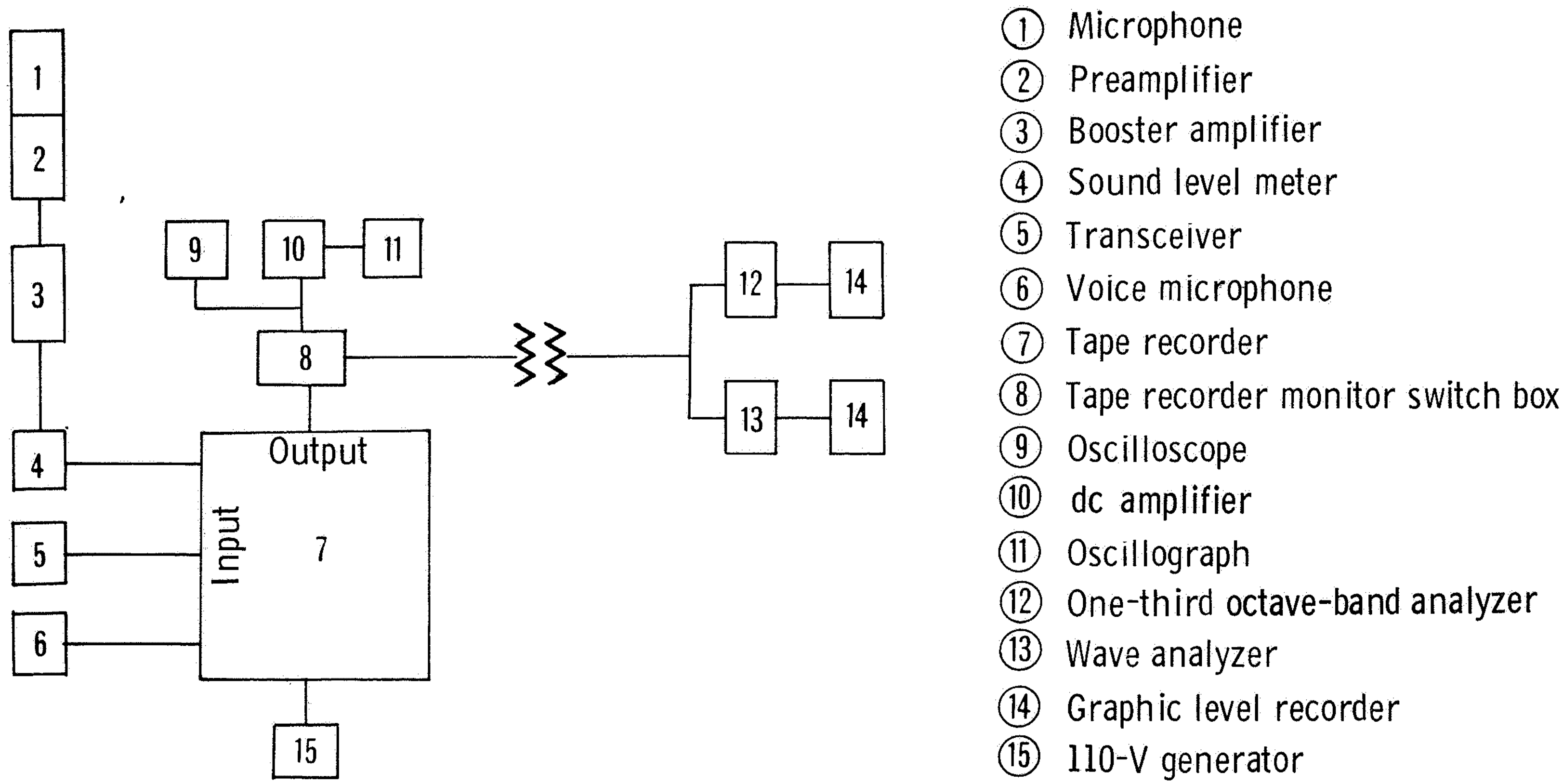

Figure 5.- Block diagram showing typical system layout for noise data acquisition and preliminary data reduction.

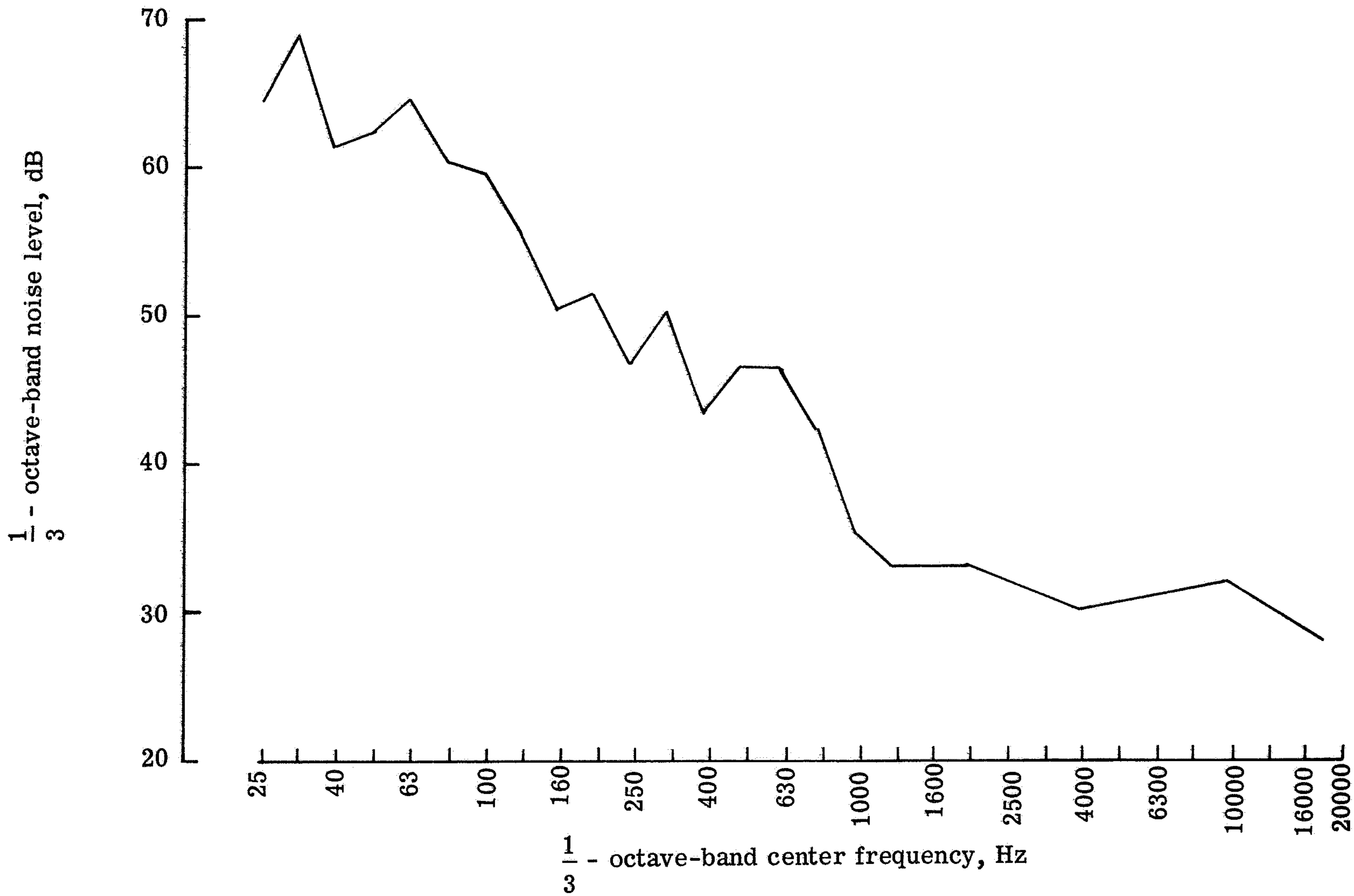

Figure 6.- Typical noise spectrum at microphone 1.

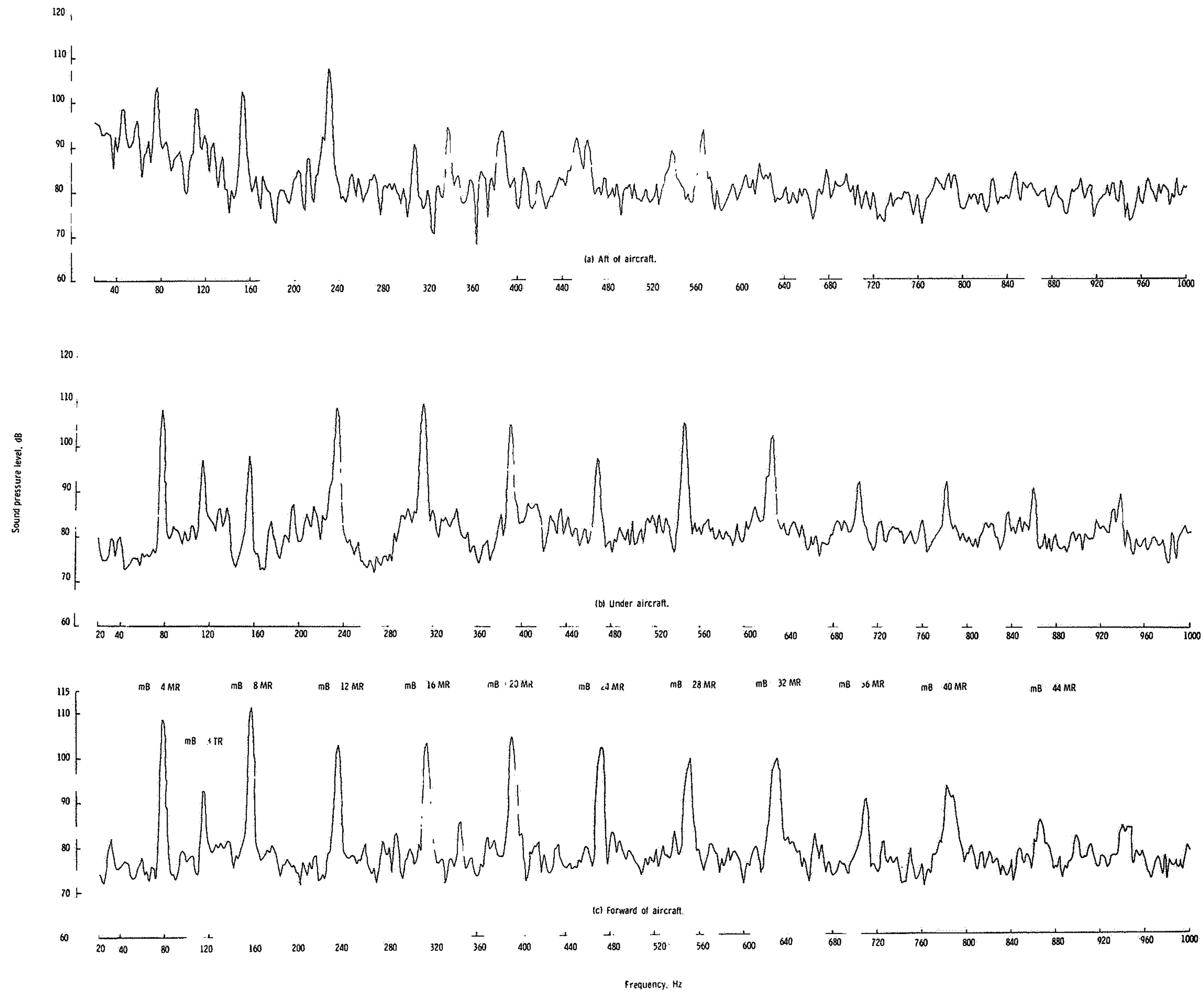

Figure 7.- On-track flyover noise spectra at airspeed of 10 knots and altitude of 79 m.

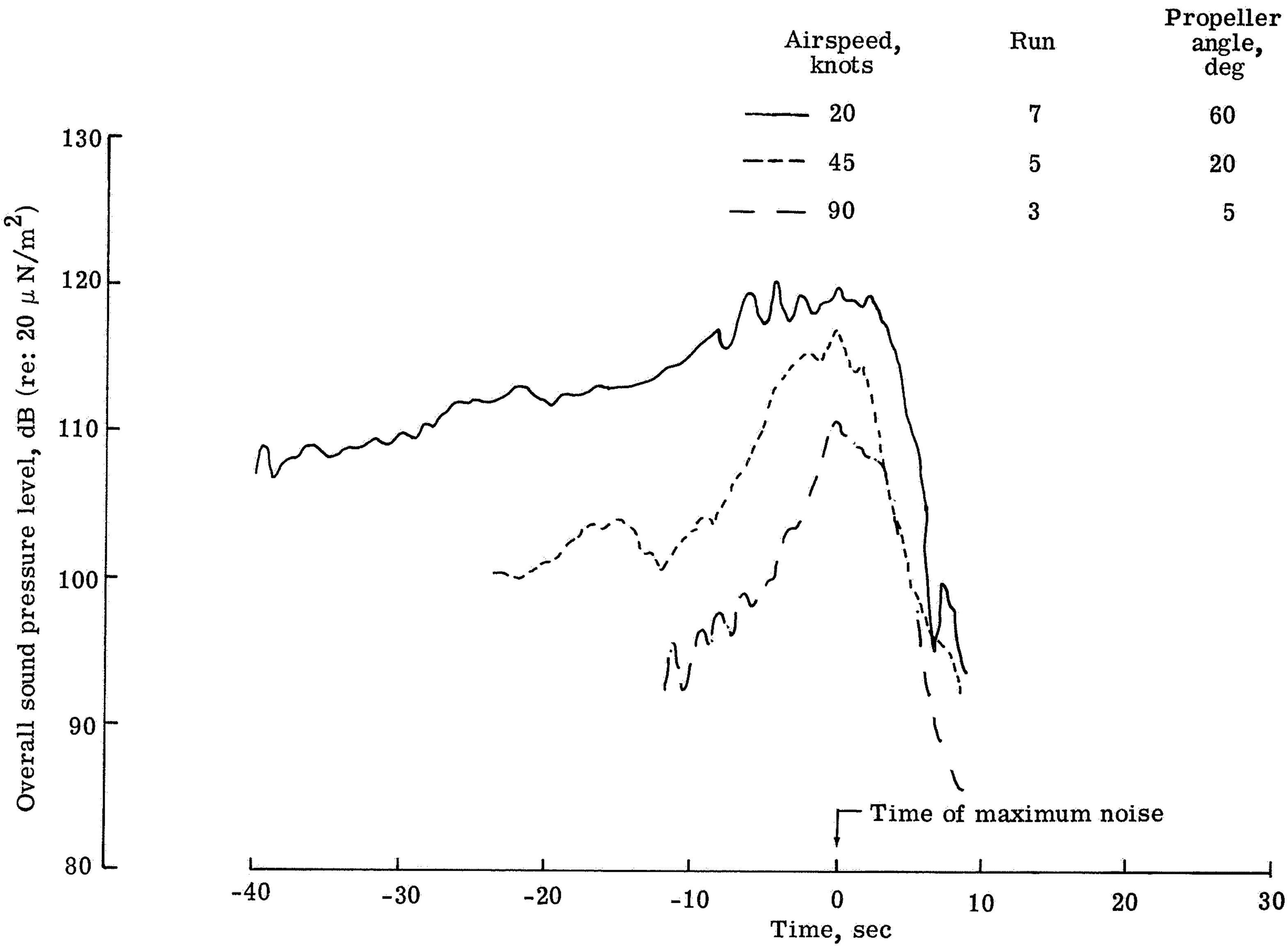

Figure 8.- Time history of on-track overall sound pressure levels during level flyovers at three airspeeds and a corrected altitude of 91 m.

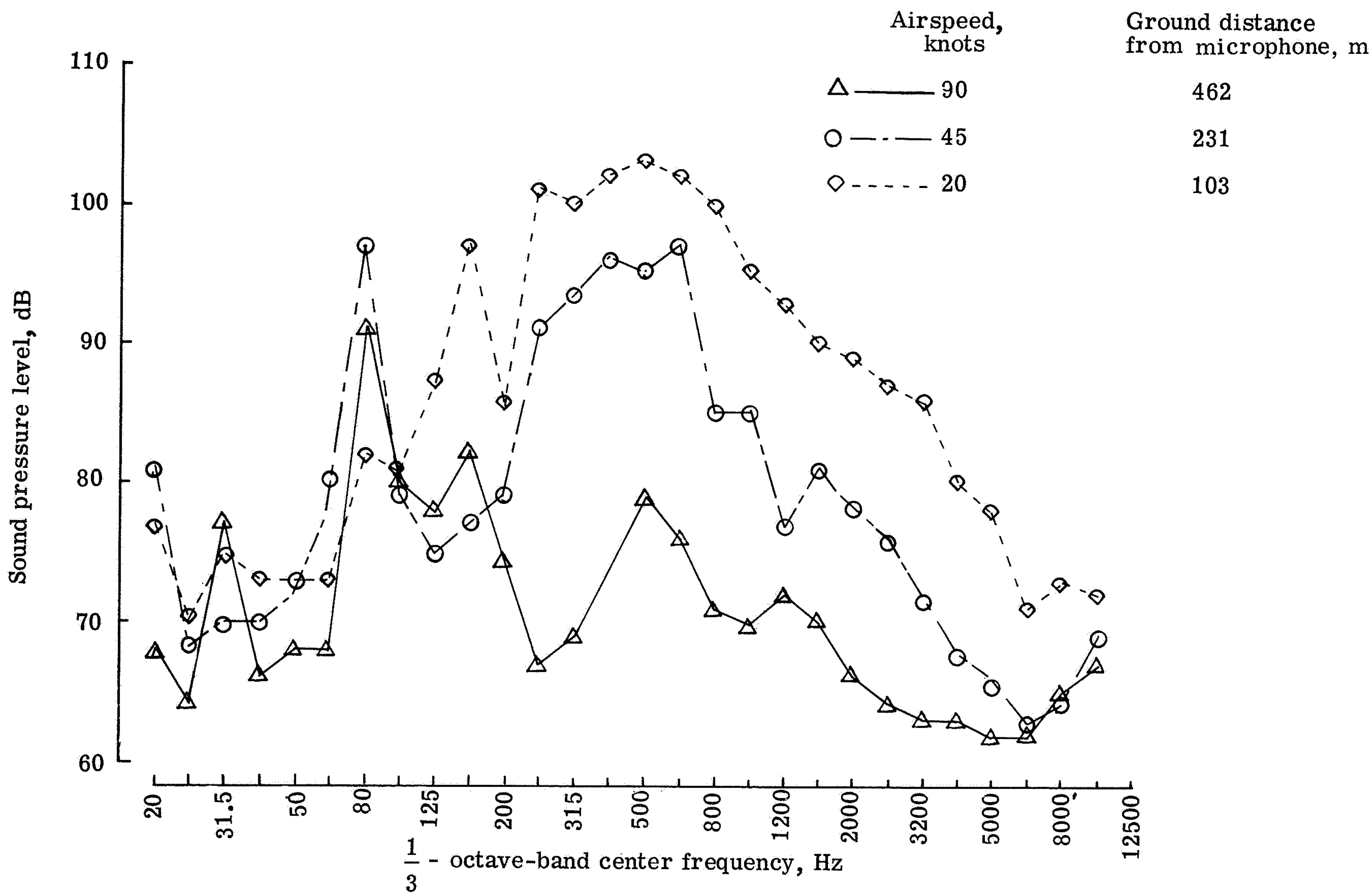

(a) 10 sec before overhead.

Figure 9.- On-track noise spectra at various times from overhead at three airspeeds and an altitude of approximately 90 m.

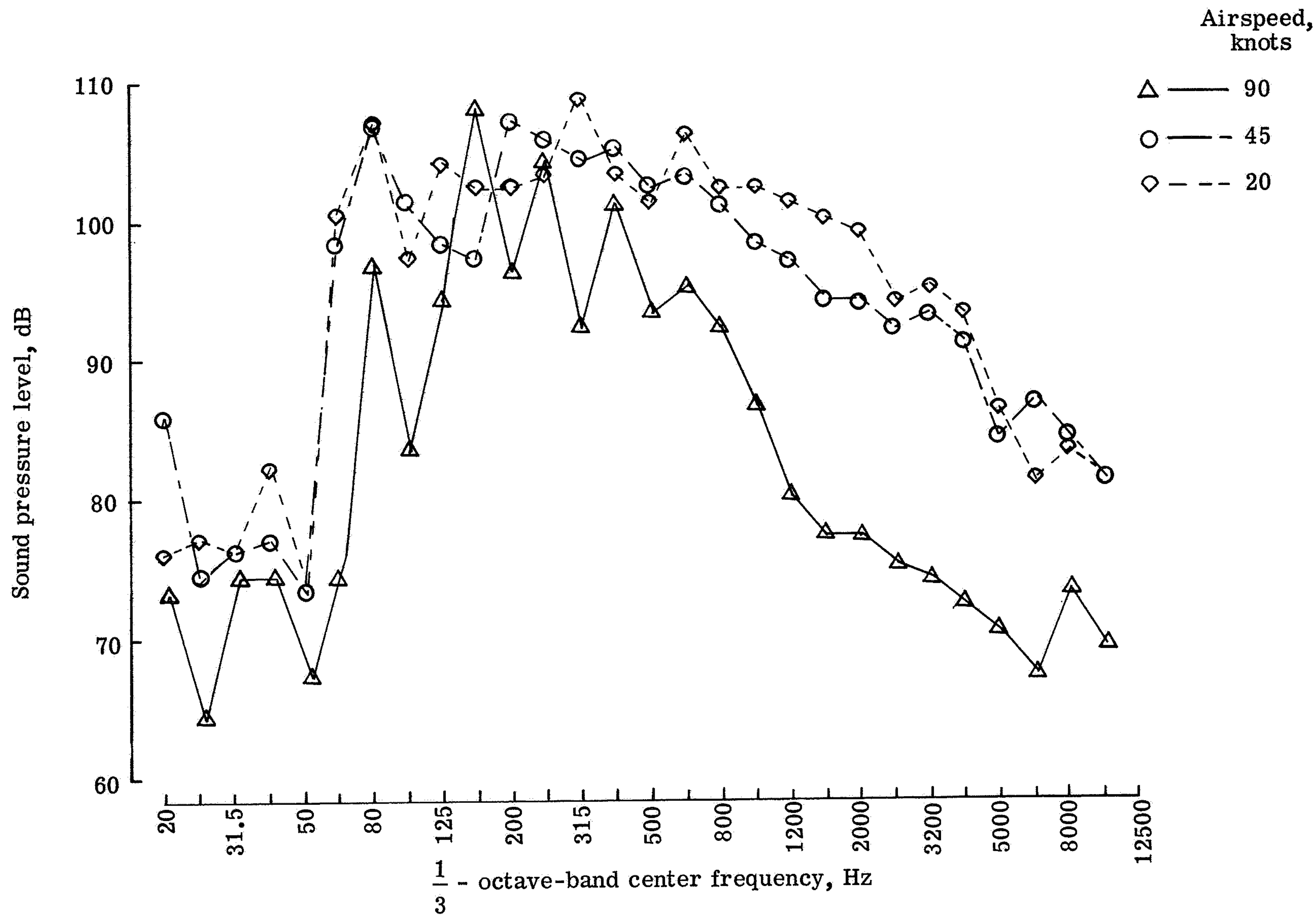

(b) Overhead.

Figure 9.- Continued.

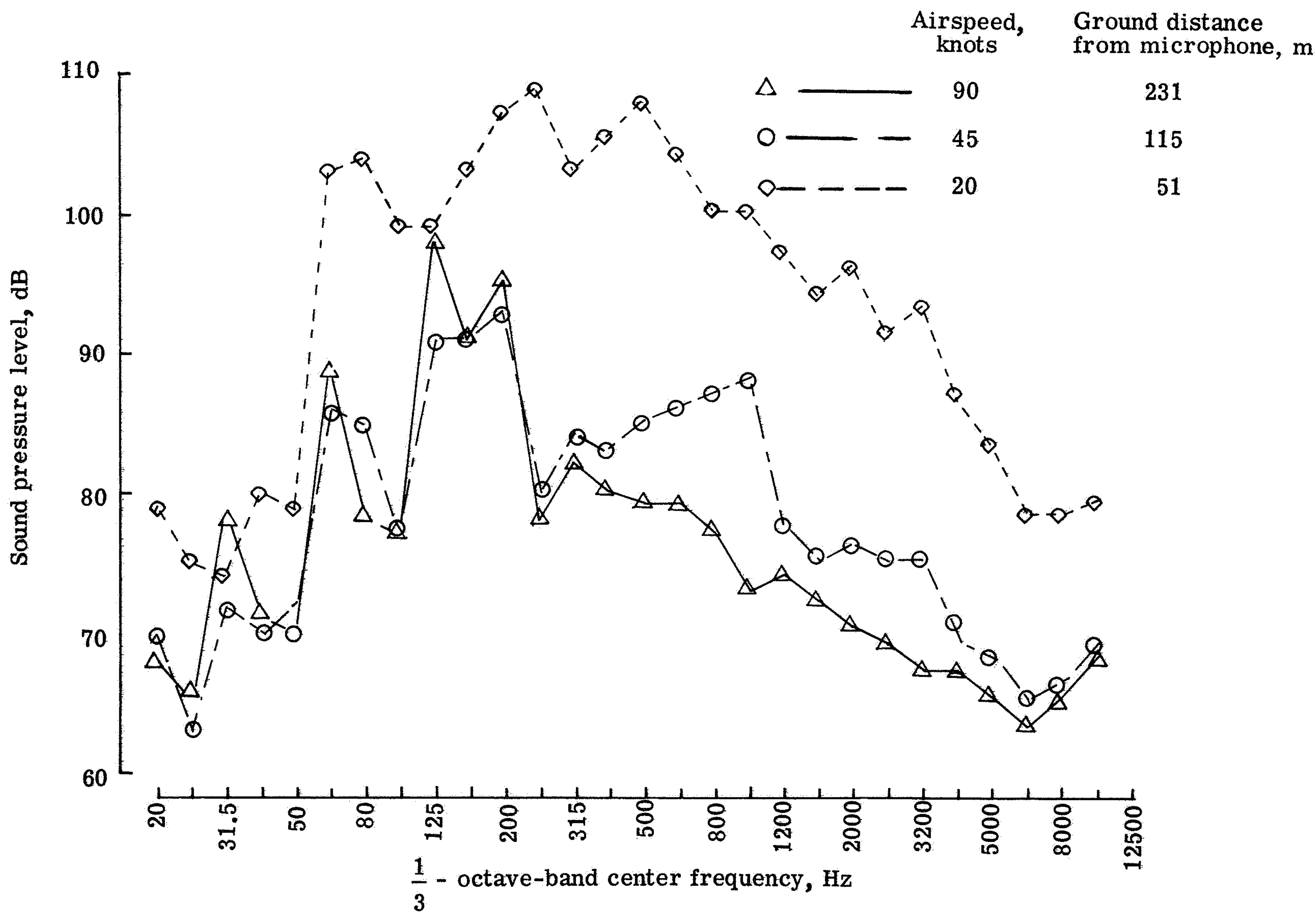

(c) 5 sec after overhead.

Figure 9.- Concluded.

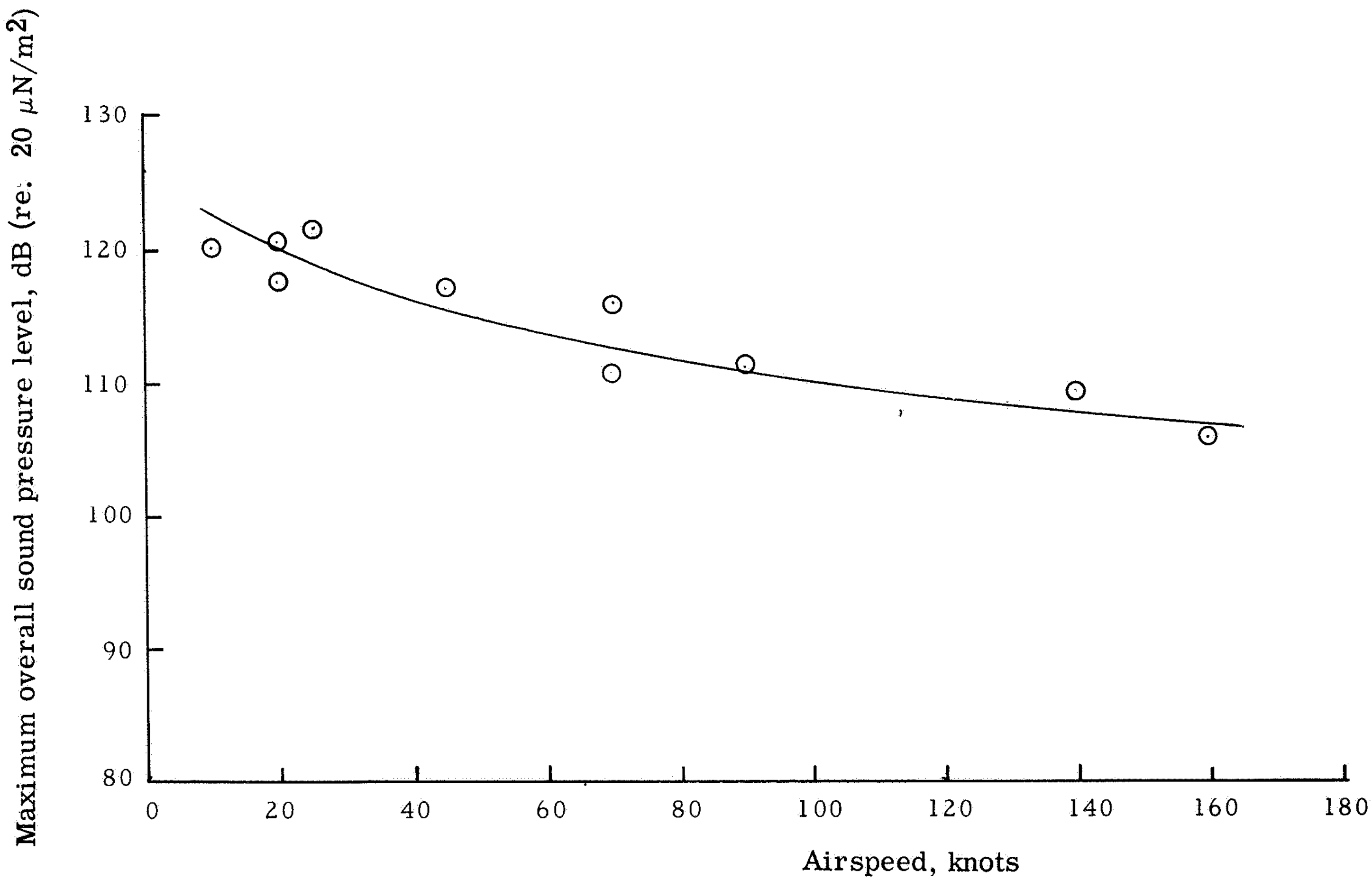

Figure 10.- Variation of maximum overall sound pressure level with airspeed at corrected altitude of 91 m.

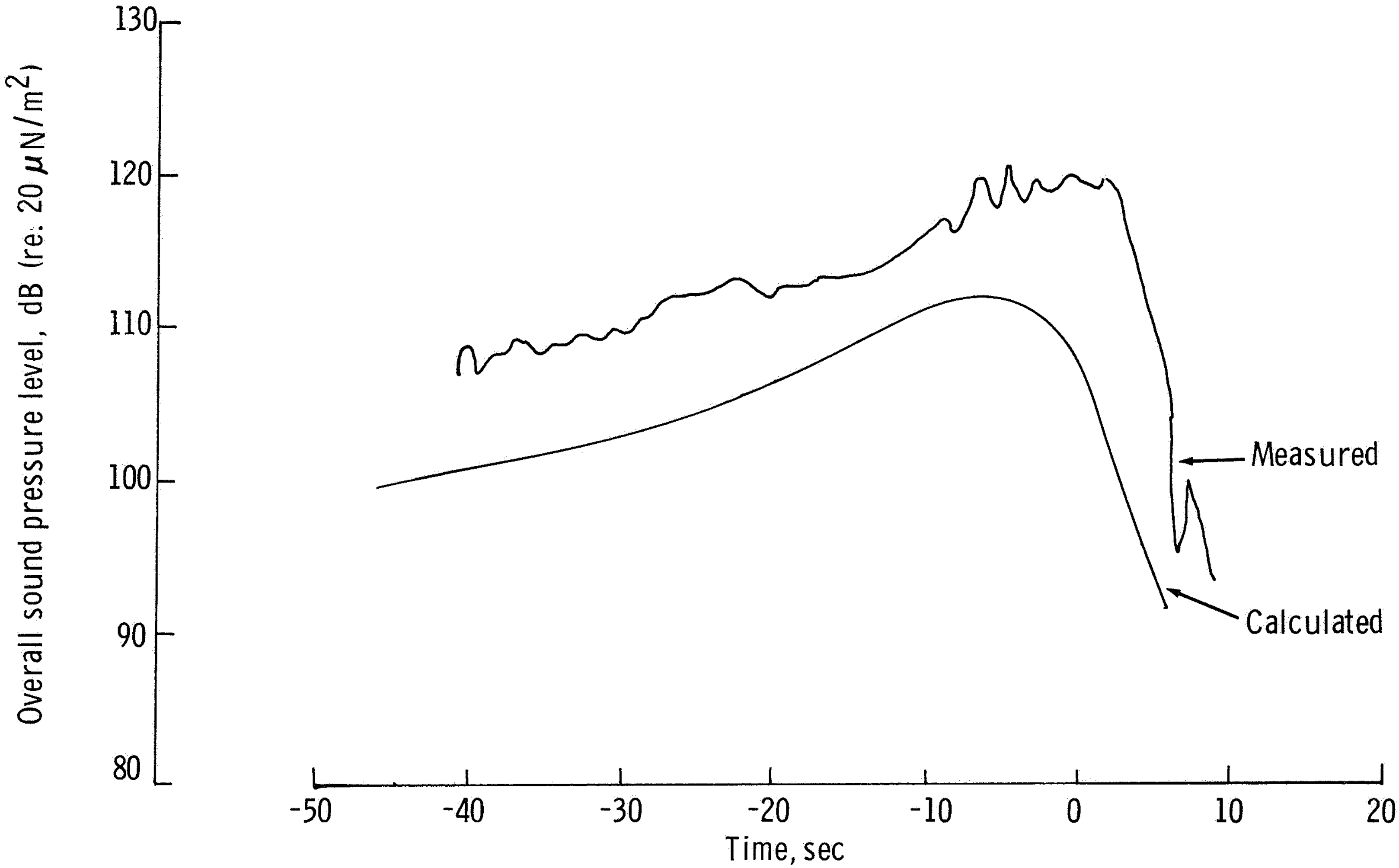

(a) Airspeed, 20 knots.

Figure 11.- Comparison of measured and calculated sound pressure levels.

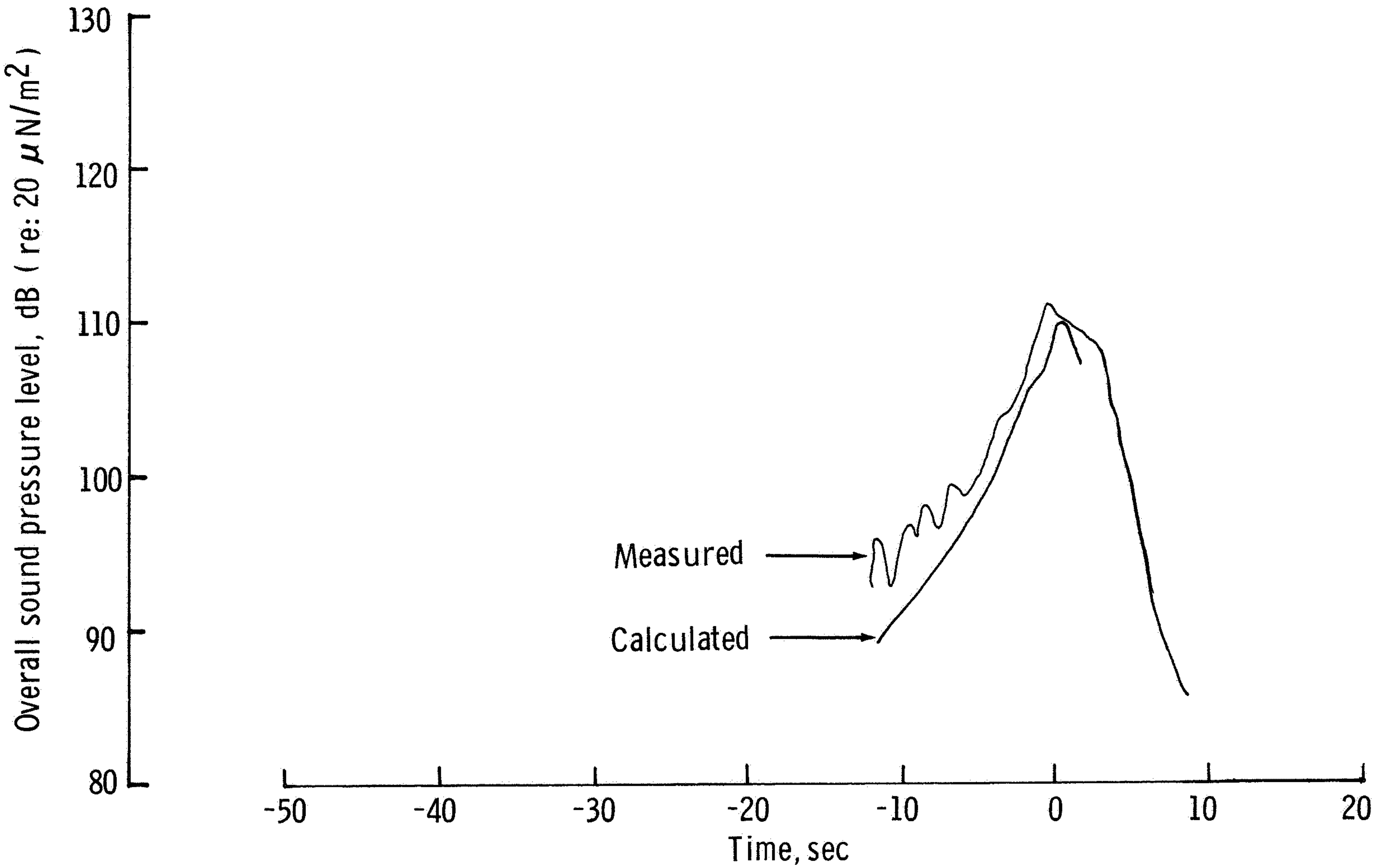

(b) Airspeed, 90 knots.

Figure 11.- Concluded.

NASA-Langley, 1974 L-9037